Exploring High Transition Temperature Superconductivity in a Freestanding or $SrTiO_3$-Supported CoSb Monolayer

Wenjun Ding,[1] Jiang Zeng,[1] Wei Qin,[1] Ping Cui,[1,2,*] and Zhenyu Zhang[1,†]
[1]International Center for Quantum Design of Functional Materials (ICQD), Hefei National Laboratory for Physical Sciences at Microscale, and Synergetic Innovation Center of Quantum Information and Quantum Physics, University of Science and Technology of China, Hefei, Anhui 230026, China
[2]Key Laboratory of Strongly-Coupled Quantum Matter Physics, Chinese Academy of Sciences, School of Physical Sciences, University of Science and Technology of China, Hefei, Anhui 230026, China

(Received 21 January 2019; revised manuscript received 5 September 2019; published 17 January 2020)

As a two-dimensional entity, FeSe has been widely explored to harbor high transition temperature (high-T_c) superconductivity in diverse physical settings; yet to date, the underlying superconducting mechanisms are still under active debate. Here we use first-principles approaches to identify a chemically different yet structurally identical counterpart of FeSe, namely, monolayered CoSb, which is shown to be an attractive candidate to harbor high-T_c superconductivity as well. We first show that a freestanding CoSb monolayer can adopt the FeSe-like layered structure, even though its known bulk phase has no resemblance to layering. Next, we demonstrate that such a CoSb monolayer possesses superconducting properties comparable with or superior to FeSe, a striking finding that can be attributed to the isovalency nature of the two systems. More importantly, the layered CoSb structure can be stabilized on $SrTiO_3(001)$, offering appealing alternative platforms for realizing high-T_c superconductivity beyond the well-established Cu- and Fe-based superconducting families. $CoSb/SrTiO_3(001)$ also exhibits distinctly different magnetic properties from $FeSe/SrTiO_3(001)$, which should provide a crucial new angle to elucidate the microscopic mechanisms of superconductivity in these and related systems.

DOI: 10.1103/PhysRevLett.124.027002

Over the last decades, tremendous advances have been made in discovering new superconductors with high superconducting transition temperatures (T_c). The cuprates [1,2] and iron-based superconductors [3–6] represent two of the best established superconductor families. Among the Fe-based superconductors, a compelling building block is the FeSe monolayer, which has been widely explored to harbor amazingly rich superconducting characteristics under otherwise diverse physical conditions [7–16]. In particular, the relatively simple atomic structure and two-dimensional (2D) nature of FeSe render versatile tunability on its superconducting properties, for example, by placing it on proper polar oxide substrates [10–13], or by stacking it into superlattice structures [9,14–16], both approaches resulting in substantially enhanced T_c. These experimental advances have also stimulated significant research efforts on revealing the underlying superconducting mechanisms involved in these systems [17–24], and such improved understanding may further lead to discoveries of new superconducting materials with potentially even higher T_c's.

Indeed, substantial efforts have also been made in searching for new high-T_c superconducting systems. In this regard, a comprehensive study has been carried out, seeking new superconductors out of over 1000 candidate systems, but none of the over 100 superconducting materials identified exhibited high-T_c superconductivity beyond the two known Cu- and Fe-based families [25]. In those earlier searches, attentions were mainly focused on materials with layered bulk structures [25]. On the other hand, more recent studies have shown that materials that do not prefer layering in bulk phases may also be stabilized as monolayers in the 2D limit [26,27]. These latest developments in the vibrant field of 2D materials effectively broaden our candidate materials space as we select monolayered systems that might exhibit high-T_c superconductivity.

In this Letter, we use first-principles approaches to identify a chemically different yet structurally identical counterpart of FeSe, namely, monolayered CoSb, which is shown to be an attractive candidate to harbor high-T_c superconductivity. We first show that a freestanding CoSb monolayer can adopt the FeSe-like layered structure, even though its known bulk phase has no resemblance to layering [28,29]. Next, we demonstrate that such a CoSb monolayer possesses superconducting properties comparable with or even superior to FeSe, a striking finding that can be attributed to the isovalency nature of the two systems. The superior aspect is partly reflected by the ~30% increase in the electron-phonon coupling (EPC) strength of the CoSb monolayer over that of the FeSe monolayer, as the EPC can be a dominant factor in such

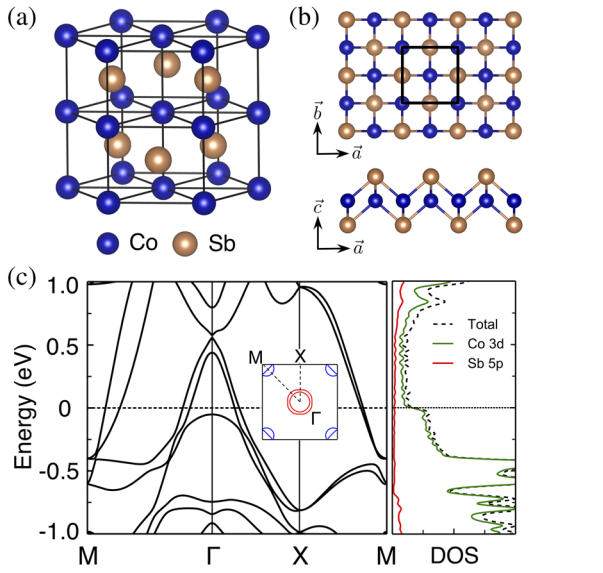

FIG. 1. Schematic atomic structures of the (a) NiAs-type bulk CoSb and (b) PbO-type monolayered CoSb. In (b), the upper and lower panel shows the top and side view, respectively. (c) Electronic structure (left panel) and density of states (DOS) (right panel) of a freestanding CoSb monolayer, with the Fermi level set at zero. The inset shows the first Brillouin zone, with the high symmetry points of Γ, M, and X indicated. The two hole pockets around the Γ point and two electron pockets around the M point are colored in red and blue, respectively.

superconducting systems [19–24]. More importantly, the layered CoSb structure can be readily stabilized on $SrTiO_3(001)$, offering appealing alternative platforms for realizing high-T_c superconductivity. Another salient and fundamentally significant feature to be emphasized is that $CoSb/SrTiO_3(001)$ exhibits distinctly different magnetic properties from $FeSe/SrTiO_3(001)$, which should provide a crucial new angle to elucidate the microscopic mechanisms of superconductivity in these and related systems.

Our important and powerful design principle in searching for new superconductors based on layered materials is isovalency, namely, chemically close systems that also preserve the same number of valence electrons as FeSe. The underlying rationale of this principle is rooted in the belief that superconductivity boils down to be executed by the correlated electrons around the Fermi level; therefore, if we essentially preserve the total number of valence electrons (namely, isovalency), while tuning other important physical factors (such as the correlation effects and magnetic properties, both of which depend on the number of d electrons involved), we may discover new superconductors with potentially higher T_c. Since superconductivity is usually harbored in the planes containing the transition metal ions such as Cu and Fe, we first replace Fe by Co in our search. Based on the isovalency rule, it is then natural to replace Se by group V elements, and one preferred element is antimony, because it also possesses stronger spin-orbit coupling (SOC) and therefore offers more opportunities for potential topological properties in addition to superconductivity [30–32]. While bulk FeSe prefers the tetragonal PbO-type layered structure, making it easier to be stabilized as a freestanding or supported FeSe monolayer, bulk CoSb prefers the NiAs-type structure with no resemblance to layering [28,29], as shown in Fig. 1(a) and Fig. S1, with more discussions presented in the Supplemental Material [33]. Nevertheless, given the isovalency nature of the two systems, we still expect that the PbO-type layered structure of CoSb is to be stabilized in the 2D limit, as confirmed below.

First, the energetic, dynamic, and thermodynamic stabilities of a freestanding PbO-type CoSb monolayer as shown in Fig. 1(b) are verified via structural optimization, phonon dispersion analysis, and *ab initio* molecular dynamics (AIMD) simulations. In doing so, we consider three initial structural configurations of a CoSb monolayer: one is the layered PbO-type structure, while the other two are directly truncated from the NiAs-type bulk phase (see Fig. S2 in the Supplemental Material [33], which contains more calculation details together with the relevant references involved [34–50]). Our calculations show that the most stable structure is the layered PbO type, with the lattice constants of $a = b = 3.75$ Å and the cohesive energy of 10.89 eV (or 7.57 eV with respect to magnetic Co and Sb) per CoSb formula unit. The two nearly degenerate NiAs-type bulk truncated structures are higher in energy by 0.77 eV. Hereafter, the use of a CoSb monolayer is always assumed to possess the PbO-type structure. As shown in Fig. 2 and Fig. S3 in the Supplemental Material [33], the phonon spectra of the CoSb monolayer have also been calculated, respectively, by using the density functional perturbation theory (DFPT) and finite displacement method, with no imaginary

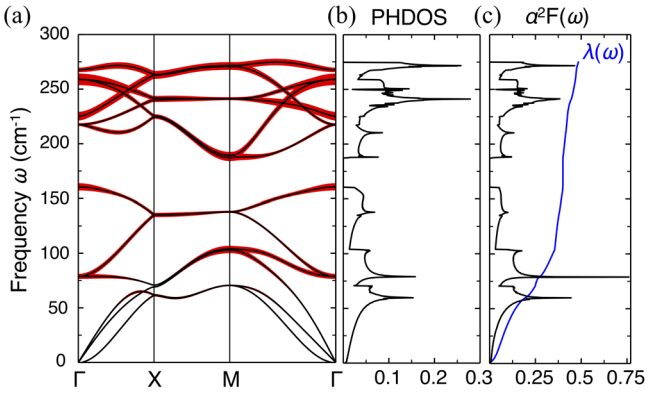

FIG. 2. (a) Phonon spectra of a freestanding CoSb monolayer calculated by using DFPT, with the magnitudes of the phonon linewidths indicated by the data sizes in red. (b) The corresponding phonon density of states (PHDOS). (c) Eliashberg function $\alpha^2F(\omega)$ (black) and frequency-dependent electron-phonon coupling $\lambda(\omega)$ (blue) of the system.

frequency detected in either approach, indicating that the system is dynamically stable. Moreover, our AIMD simulations at 100 K and up to 3 ps demonstrate that the CoSb monolayer is thermodynamically stable as well (see Fig. S4 in the Supplemental Material [33]).

The electronic structure of the CoSb monolayer obtained within the generalized gradient approximation (GGA) scheme and with the inclusion of the SOC is displayed in Fig. 1(c), showing that the system is metallic, and possesses very similar behaviors to that of the FeSe monolayer (as compared in Fig. S5 of the Supplemental Material [33]). The density of states (DOS) around the Fermi level is mainly contributed by the $3d$ orbitals of the Co atoms, as confirmed by the projected density of states (PDOS) shown in the right panel of Fig. 1(c). In particular, there are two hole pockets around the Γ point and two electron pockets around the M point in the first Brillouin zone, and those features were also revealed in theoretical studies of the freestanding FeSe monolayer [51]. These close similarities in the electronic structures between the CoSb and FeSe monolayers are again attributable to their isovalency, and may result in comparable superconducting properties in the two systems as well.

Next, we turn our attention to the superconducting properties of the CoSb monolayer. As we know, the dominant pairing mechanisms in the FeSe-based superconducting systems have been actively debated, with antiferromagnetic fluctuations [17,18], EPC [19–24], or the resultant effect of the two [19,22] to be frequently invoked. Here we use the EPC strength as a quantitative indicator for superconductivity, especially because more recent studies have strongly supported its importance in enhancing the T_c's of the FeSe-based superconductors [19–24]. The EPC strength λ can be calculated from the isotropic version of the Eliashberg function $\alpha^2F(\omega)$ as [43,44]:

$$\lambda = 2\int_0^\infty \frac{\alpha^2F(\omega)}{\omega}d\omega, \tag{1}$$

where ω is the phonon frequency. As shown in Fig. 2, for the CoSb monolayer, $\lambda_{\mathrm{CoSb}} = 0.48$, which is ~1.3 times larger than that of the FeSe monolayer within otherwise identical computational accuracy ($\lambda_{\mathrm{FeSe}} = 0.38$, as compared in Fig. S6 of the Supplemental Material [33]). To further estimate T_c, we use the McMillan-Allen-Dynes parametrized Eliashberg equation [43,44,52],

$$k_BT_c = \frac{\hbar\omega_{\log}}{1.2}\exp\left(-\frac{1.04(1+\lambda)}{\lambda-\mu^*(1+0.62\lambda)}\right), \tag{2}$$

$$\omega_{\log} = \exp\left(\frac{2}{\lambda}\int_0^\infty d\omega\frac{\alpha^2F(\omega)}{\omega}\log\omega\right), \tag{3}$$

where $\omega_{\log}$ is the logarithmic average of the phonon frequencies, while μ^* is a parameter describing the Coulomb repulsion, which usually takes values in the range of 0.1–0.2 [52]. By choosing μ^* as 0.1, the T_c of the freestanding CoSb monolayer is estimated to be 0.9 K, higher than the estimated T_c of 0.5 K for the FeSe monolayer, indicating comparable or superior superconducting properties based on the EPC scheme alone. Qualitatively, the higher T_c for the freestanding CoSb monolayer can be attributed to the phonon softening (see Fig. S7 in the Supplemental Material [33]), which leads to a compensation effect on T_c.

The next, and more crucial, issue is to investigate the behaviors of the CoSb monolayer on the $SrTiO_3$ (STO) substrate, especially with regard to achieving high-T_c superconductivity. When a CoSb monolayer is laid epitaxially on $SrTiO_3(001)$ (CoSb/STO), three high-symmetry stacking configurations are considered (see Fig. S8 in the Supplemental Material [33]). Figure 3(a) shows energetically the most stable structure, where the bottom Sb atoms of CoSb sit directly on top of the surface Ti atoms of the STO with an interlayer spacing of 3.0 Å. The other two configurations are at least 0.04 eV higher in energy per CoSb formula unit (see Table S1 in the Supplemental Material [33]). The binding energy of the heterostructure is further defined as $E_b = E_{\mathrm{STO}} + E_{\mathrm{CoSb}} - E_{\mathrm{CoSb/STO}}$, where E_{STO}, E_{CoSb}, and $E_{\mathrm{CoSb/STO}}$ are the total energies of STO, CoSb, and CoSb/STO, respectively. For the most stable structure, $E_b = 0.28$ eV per CoSb formula unit, indicating a relatively weak interlayer coupling. Furthermore, our AIMD simulations at 100 K and up to 3 ps show that the structure shown

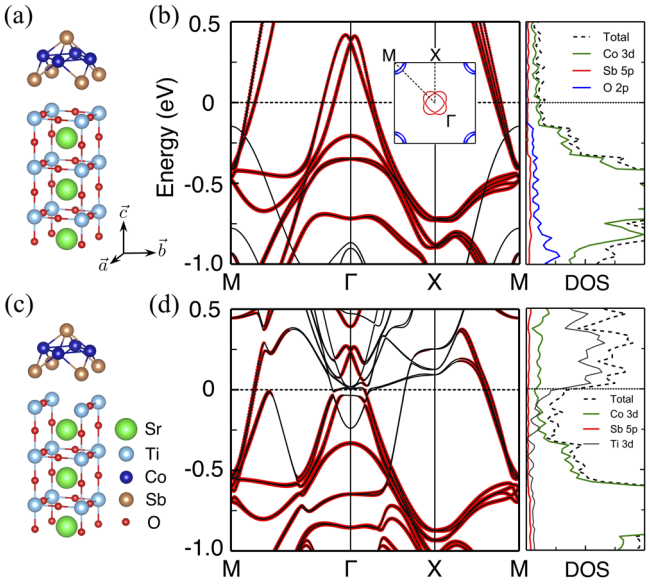

FIG. 3. Atomic structures of a CoSb monolayer on (a) ideal and (c) surface-oxygen-deficient $SrTiO_3(001)$ substrates. (b),(d) Electronic structures (left panels) and DOS (right panels) of the corresponding systems. The Fermi level is set at zero. The spectral weights contributed by the CoSb overlayers are indicated by the data sizes in red. The inset in (b) shows the Fermi surface in the first Brillouin zone.

in Fig. 3(a) is also thermodynamically stable (see Fig. S9 in the Supplemental Material [33]).

The band structure of the most stable CoSb/STO system is depicted in Fig. 3(b). In analogy to the freestanding CoSb monolayer [Fig. 1(c)], here CoSb/STO is preserved to be metallic, possessing two hole pockets around the Γ point and two electron pockets around the M point. Since the Fermi level is located in the band gap of the STO substrate, the DOS around the Fermi level is still dominated by the contributions from the $3d$ orbitals of the Co atoms, as confirmed by the PDOS shown in Fig. 3(b). The charge transfer between the CoSb overlayer and STO substrate is negligible due to their relatively weak (or van der Waals-type) interaction. These electronic properties again share great similarities with that of the FeSe/STO system [51,53] (also see Fig. S10 in the Supplemental Material [33]), strongly suggesting comparable superconducting properties as well.

For the reference system of FeSe/STO, it has also been well established that significant charge transfer from the substrate to the FeSe overlayer must take place to achieve high T_c [54–59]. Furthermore, the presence of oxygen vacancies in the STO substrates is one of the effective schemes for inducing charge transfer [57–59]. Here we investigate the interfacial charge transfer in CoSb/STO by introducing surface oxygen vacancies into the STO substrate, as shown in Fig. 3(c). As expected, the creation of an oxygen vacancy leads to structural and energetic changes at the interface, shortening the interlayer spacing to 2.9 Å and increasing the binding energy to 0.54 eV per CoSb formula unit. Such an enhanced interlayer coupling is accompanied by pronounced charge transfer from the STO to CoSb, reflected by the downward shift in the energy bands of CoSb shown in Fig. 3(d). Detailed calculations confirm that the amount of charge transfer from the STO to CoSb is ∼0.060 e per CoSb formula unit, qualitatively similar to that of the FeSe/STO systems [58,59] (see Fig. S11 in the Supplemental Material [33]).

Even though the dominant superconducting mechanisms for the high-T_c superconductivity in FeSe/STO are still unclear, recent studies have pointed to several crucial and consensus ingredients. First, the overlayer itself or its bulk form should be superconducting [7]. Second, as mentioned earlier, significant charge transfer from the substrate to the FeSe overlayer is indispensable [54–57,60,61], which also appears as an important factor in other types of FeSe-based high-T_c superconductors [15,16]. Third, the longitudinal optical phonons of the STO are able to penetrate into the FeSe overlayer [62], which is then expected to enhance the superconductivity via stronger electron pairing [19,23]. Based on the present study, CoSb/STO possesses all these essential ingredients, thereby strongly favoring the system to serve as a highly appealing new platform for realizing high-T_c superconductivity beyond the FeSe-based systems.

Aside from the dominant superconducting enhancement mechanisms, even less is known about the intrinsic pairing mechanisms in the FeSe overlayer. Earlier theoretical studies had emphasized antiferromagnetic spin fluctuations to be potentially dominating [17,18]. More recently, the EPC has been increasingly recognized as the dominant microscopic origin of superconductivity with variable T_c's [20,23,24]. Since both FeSe and CoSb largely form covalent bonds due to comparable electronegativities (namely, Fe: 1.83 versus Se: 2.55, and Co: 1.88 versus Sb: 2.05), the different numbers of valence d electrons participating in the covalent bonding formation will be inherently manifested in the resulting monolayers. Such a difference in $3d$ electrons will likely make CoSb/STO highly desirable to exhibit new physics different from FeSe/STO, especially on the magnetic properties.

To explore this point, we start with the energetically stable structure of both CoSb/STO [Fig. 3(a)] and FeSe/STO [51], and consider four typical magnetic configurations, namely, the nonmagnetic (NM), ferromagnetic (FM), collinear antiferromagnetic (CAFM), and Néel antiferromagnetic (NAFM), as shown in Fig. 4(a). In our calculations, we use an on-site Hubbard U as the empirical parameter to describe the correlation effects associated with the $3d$ electrons. The magnetic moment M of the transition metal atoms (Fe or Co) as a function of U is compared in Figs. 4(b) and 4(c), together with the relative energy ΔE of the four magnetic configurations measured by $\Delta E = E - E_{\mathrm{CAFM}}$, where E and E_{CAFM} are the total energies of a given magnetic and CAFM configurations, respectively. Indeed, we find that at $U = 0$, the ground state of the CoSb/STO is NM, with $M = 0$ [see Fig. 4(b)]; in contrast, the ground state of the FeSe/STO is the CAFM state, with $M = 2.4\ \mu_B$ per Fe atom [see Fig. 4(c)]. Furthermore, M is finite only when $U > 2$ eV, and saturates at $\sim 2\ \mu_B$ per Co, while M varies within $(2 \sim 4)$

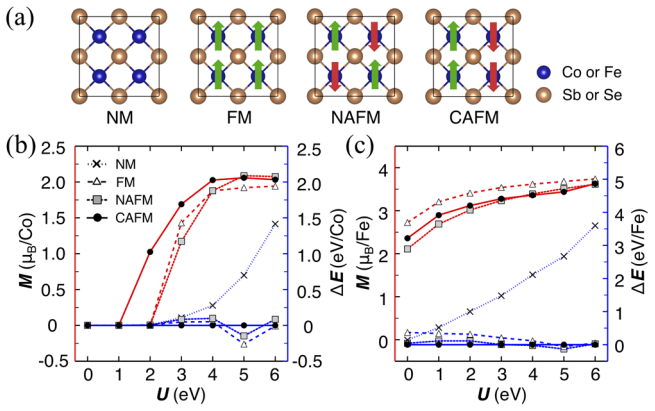

FIG. 4. (a) Four commonly considered magnetic configurations of CoSb/STO or FeSe/STO. (b),(c) Dependences of the magnetic moment M (red) and relative energy ΔE (blue) of the four magnetic configurations as functions of the on-site Hubbard U for the two systems.

μ_B per Fe, depending on the specific magnetic configurations. These major differences can be qualitatively attributed to the overall more delocalized nature of electrons in the CoSb than FeSe, and can provide a crucial new angle to elucidate the dominant microscopic mechanisms of superconductivity in these and related systems. Specifically, if CoSb/STO is definitively confirmed to be a high-T_c system, it will provide a key piece of evidence to exclude the spin-fluctuation mechanism as the dominant one. In contrast, if CoSb/STO is not a high-T_c system, the finding should offer complementary support to the spin-fluctuation mechanism. Such new insights may lead to distinct differentiations between the dominant competing mechanisms of superconductivity.

We have also examined the double stripe antiferromagnetic (Bi-CAFM: bicollinear antiferromagnetic) configuration [48–50] for both CoSb/STO and FeSe/STO, and the trends stay intact (see Fig. S12 in the Supplemental Material [33]). Furthermore, by employing a Heisenberg model [48] together with the first-principles results, the nearest (J_1), next-nearest (J_2), and next-next-nearest (J_3) neighboring magnetic couplings in CoSb/STO can be extracted, with the results of $U = 0$ or 3 eV given in the Supplemental Material [33] (see Fig. S13 and Table S2).

Here we also note that discrepancies exist between the results of first-principles calculations and experimental observations of the electronic structures of FeSe/STO [51,54,56,57]. Such discrepancies have been predominantly attributed to limitations of first-principles approaches in describing strongly correlated electrons [21,63], and, potentially more pertinently, could also be tied to discrepancies between model systems treated in theory and realistic systems studied in experiment (as partially reflected by the uncertainties in the origin of charge transfer [12,64]). Similar computational challenges may also be faced in describing CoSb/STO, while ultimately overcoming such challenges awaits major advances in the field.

Before closing, we briefly discuss several aspects that need to be observed in potential experimental validations of the strong and innovative predictions made here. First, since the preferred bulk structure of CoSb is not layered, the deposition rate needs to be carefully controlled, to avoid growing into the 3D bulk structure. Second, given the specific atomic arrangements of the CoSb monolayer in the PbO-type structure, it may be desirable to grow Sb first, followed by proper amounts of Co and Sb. Third, our detailed AIMD simulations have shown that the CoSb/STO heterostructure is stable at least up to 100 K, suggesting that the growth process can be made within a comparable temperature range.

In summary, following the isovalency rule, we have predicted a chemically different yet structurally identical counterpart of monolayered FeSe, namely, monolayered CoSb, as a highly appealing candidate for harboring high-T_c superconductivity beyond the well-established Cu- and Fe-based superconductor families. Our comprehensive studies have shown that the freestanding CoSb monolayer is energetically, dynamically, and thermodynamically stable, even though its known bulk phase has no resemblance to layering. Such an identification of a new 2D material beyond the expectation of the big materials database [25,65,66] is intriguing and significant in its own right. More strikingly, the electronic structures of the CoSb monolayer either in freestanding form or supported on STO share great similarities with the FeSe counterparts, strongly indicating that the system can also be tuned into a high-T_c superconductor [67]. Furthermore, CoSb/STO exhibits distinctly different magnetic properties from FeSe/STO, which can be exploited to identify the dominant microscopic mechanisms of high-T_c superconductivity in these and related systems.

This work was supported by the National Key R&D Program of China (Grant No. 2017YFA0303500), the National Natural Science Foundation of China (Grants No. 11634011, No. 61434002, No. 11722435, and No. 11974323), the Strategic Priority Research Program of Chinese Academy of Sciences (Grant No. XDB30000000), the Anhui Initiative in Quantum Information Technologies (Grant No. AHY170000), and China Postdoctoral Science Foundation (Grant No. BH2340000106).

Note added.—Recently, several experimental groups have been motivated to test our predictions, and their preliminary results show that CoSb monolayered films with different symmetries can indeed be grown on STO(001); furthermore, these films exhibit sizable (namely, high-T_c) superconductinglike gaps, as observed by scanning tunneling spectroscopy [67,68].

*Corresponding authors.
cuipg@ustc.edu.cn
†Corresponding authors.
zhangzy@ustc.edu.cn

[1] J. G. Bednorz and K. A. Müller, Z. Phys. B **64**, 189 (1986).
[2] A. Damascelli, Z. Hussain, and Z.-X. Shen, Rev. Mod. Phys. **75**, 473 (2003).
[3] Y. Kamihara, H. Hiramatsu, M. Hirano, R. Kawamura, H. Yanagi, T. Kamiya, and H. Hosono, J. Am. Chem. Soc. **128**, 10012 (2006).
[4] Y. Kamihara, T. Watanabe, M. Hirano, and H. Hosono, J. Am. Chem. Soc. **130**, 3296 (2008).
[5] X. H. Chen, T. Wu, G. Wu, R. H. Liu, H. Chen, and D. F. Fang, Nature (London) **453**, 761 (2008).
[6] J. Paglione and R. L. Greene, Nat. Phys. **6**, 645 (2010).
[7] F.-C. Hsu, J.-Y. Luo, K.-W. Yeh, T.-K. Chen, T.-W. Huang, P. M. Wu, Y.-C. Lee, Y.-L. Huang, Y.-Y. Chu, D.-C. Yan *et al.*, Proc. Natl. Acad. Sci. U.S.A. **105**, 14262 (2008).

[8] S. Medvedev, T. M. McQueen, I. A. Troyan, T. Palasyuk, M. I. Eremets, R. J. Cava, S. Naghavi, F. Casper, V. Ksenofontov, G. Wortmann *et al.*, Nat. Mater. **8**, 630 (2009).

[9] J. Guo, S. Jin, G. Wang, S. Wang, K. Zhu, T. Zhou, M. He, and X. Chen, Phys. Rev. B **82**, 180520(R) (2010).

[10] Q.-Y. Wang, Z. Li, W.-H. Zhang, Z.-C. Zhang, J.-S. Zhang, W. Li, H. Ding, Y.-B. Ou, P. Deng, K. Chang *et al.*, Chin. Phys. Lett. **29**, 037402 (2012).

[11] R. Peng, H. C. Xu, S. Y. Tan, H. Y. Cao, M. Xia, X. P. Shen, Z. C. Huang, C. H. P. Wen, Q. Song, T. Zhang *et al.*, Nat. Commun. **5**, 5044 (2014).

[12] H. Ding, Y.-F. Lv, K. Zhao, W.-L. Wang, L. Wang, C.-L. Song, X. Chen, X.-C. Ma, and Q.-K. Xue, Phys. Rev. Lett. **117**, 067001 (2016).

[13] S. N. Rebec, T. Jia, C. Zhang, M. Hashimoto, D.-H. Lu, R. G. Moore, and Z.-X. Shen, Phys. Rev. Lett. **118**, 067002 (2017).

[14] M. Burrard-Lucas, D. G. Free, S. J. Sedlmaier, J. D. Wright, S. J. Cassidy, Y. Hara, A. J. Corkett, T. Lancaster, P. J. Baker, S. J. Blundell *et al.*, Nat. Mater. **12**, 15 (2013).

[15] X. F. Lu, N. Z. Wang, H. Wu, Y. P. Wu, D. Zhao, X. Z. Zeng, X. G. Luo, T. Wu, W. Bao, G. H. Zhang *et al.*, Nat. Mater. **14**, 325 (2015).

[16] U. Pachmayr, F. Nitsche, H. Luetkens, S. Kamusella, F. Brückner, R. Sarkar, H.-H. Klauss, and D. Johrendt, Angew. Chem. Int. Ed. **54**, 293 (2015).

[17] P. J. Hirschfeld, M. M. Korshunov, and I. I. Mazin, Rep. Prog. Phys. **74**, 124508 (2011).

[18] D. J. Scalapino, Rev. Mod. Phys. **84**, 1383 (2012).

[19] J. J. Lee, F. T. Schmitt, R. G. Moore, S. Johnston, Y.-T. Cui, W. Li, M. Yi, Z. K. Liu, M. Hashimoto, Y. Zhang *et al.*, Nature (London) **515**, 245 (2014).

[20] S. Coh, M. L. Cohen, and S. G. Louie, New J. Phys. **17**, 073027 (2015).

[21] S. Gerber, S.-L. Yang, D. Zhu, H. Soifer, J. A. Sobota, S. Rebec, J. J. Lee, T. Jia, B. Moritz, C. Jia *et al.*, Science **357**, 71 (2017).

[22] D.-H. Lee, Annu. Rev. Condens. Matter Phys. **9**, 261 (2018).

[23] S. Zhang, T. Wei, J. Guan, Q. Zhu, W. Qin, W. Wang, J. Zhang, E. W. Plummer, X. Zhu, Z. Zhang, and J. Guo, Phys. Rev. Lett. **122**, 066802 (2019).

[24] Y. L. Huang, J. Yuan, T. Wei, Z. P. Feng, W. Hu, W. Qin, J. Li, S. L. Ni, S. S. Yue, J. P. Tian *et al.* (unpublished).

[25] H. Hosono, K. Tanabe, E. Takayama-Muromachi, H. Kageyama, S. Yamanaka, H. Kumakura, M. Nohara, H. Hiramatsu, and S. Fujitsu, Sci. Technol. Adv. Mater. **16**, 033503 (2015).

[26] Z. Zhu, X. Cai, S. Yi, J. Chen, Y. Dai, C. Niu, Z. Guo, M. Xie, F. Liu, J.-H. Cho *et al.*, Phys. Rev. Lett. **119**, 106101 (2017).

[27] M. C. Lucking, W. Xie, D.-H. Choe, D. West, T.-M. Lu, and S. B. Zhang, Phys. Rev. Lett. **120**, 086101 (2018).

[28] A. Kjekshus and K. P. Walseth, Acta Chem. Scand. **23**, 2621 (1969).

[29] P. Amornpitoksuk, D. Ravot, A. Mauger, and J. C. Tedenac, Phys. Rev. B **77**, 144405 (2008).

[30] W. Qin, L. Li, and Z. Zhang, Nat. Phys. **15**, 796 (2019).

[31] P. Zhang, K. Yaji, T. Hashimoto, Y. Ota, T. Kondo, K. Okazaki, Z. Wang, J. Wen, G. D. Gu, H. Ding *et al.*, Science **360**, 182 (2018).

[32] D. Wang, L. Kong, P. Fan, H. Chen, S. Zhu, W. Liu, L. Cao, Y. Sun, S. Du, J. Schneeloch *et al.*, Science **362**, 333 (2018).

[33] See Supplemental Material at http://link.aps.org/supplemental/10.1103/PhysRevLett.124.027002, which includes Refs. [34–50], for the details of calculations and supplemental figures and tables.

[34] G. Kresse and J. Furthmüller, Phys. Rev. B **54**, 11169 (1996).

[35] P. E. Blöchl, Phys. Rev. B **50**, 17953 (1994).

[36] G. Kresse and D. Joubert, Phys. Rev. B **59**, 1758 (1999).

[37] J. P. Perdew, K. Burke, and M. Ernzerhof, Phys. Rev. Lett. **77**, 3865 (1996).

[38] M. Methfessel and A. T. Paxton, Phys. Rev. B **40**, 3616 (1989).

[39] S. Grimme, J. Antony, S. Ehrlich, and H. Krieg, J. Chem. Phys. **132**, 154104 (2010).

[40] S. L. Dudarev, G. A. Botton, S. Y. Savrasov, C. J. Humphreys, and A. P. Sutton, Phys. Rev. B **57**, 1505 (1998).

[41] P. Giannozzi, S. Baroni, N. Bonini, M. Calandra, R. Car, C. Cavazzoni, D. Ceresoli, G. L. Chiarotti, M. Cococcioni, I. Dabo *et al.*, J. Phys. Condens. Matter **21**, 395502 (2009).

[42] A. Togo and I. Tanaka, Scr. Mater. **108**, 1 (2015).

[43] W. L. McMillan, Phys. Rev. **167**, 331 (1968).

[44] P. B. Allen and R. C. Dynes, Phys. Rev. B **12**, 905 (1975).

[45] S. Nosé, J. Chem. Phys. **81**, 511 (1984).

[46] M.-G. Park, J. H. Song, J.-S. Sohn, C. K. Lee, and C.-M. Park, J. Mater. Chem. A **2**, 11391 (2014).

[47] C. Xian, Y. Wang, J. Wang, L. Zhang, Y. Han, L. Cao, and Y. Xiong, J. Supercond. Novel Magn. **31**, 1841 (2018).

[48] F. Ma, W. Ji, J. Hu, Z.-Y. Lu, and T. Xiang, Phys. Rev. Lett. **102**, 177003 (2009).

[49] J. K. Glasbrenner, I. I. Mazin, H. O. Jeschke, P. J. Hirschfeld, R. M. Fernandes, and R. Valentí, Nat. Phys. **11**, 953 (2015).

[50] M. C. Lucking, F. Zheng, M. J. Han, J. Bang, and S. Zhang, Phys. Rev. B **98**, 014504 (2018).

[51] K. Liu, Z.-Y. Lu, and T. Xiang, Phys. Rev. B **85**, 235123 (2012).

[52] F. Giustino, Rev. Mod. Phys. **89**, 015003 (2017).

[53] K. Zou, S. Mandal, S. D. Albright, R. Peng, Y. Pu, D. Kumah, C. Lau, G. H. Simon, O. E. Dagdeviren, X. He *et al.*, Phys. Rev. B **93**, 180506(R) (2016).

[54] S. He, J. He, W. Zhang, L. Zhao, D. Liu, X. Liu, D. Mou, Y.-B. Ou, Q.-Y. Wang, Z. Li *et al.*, Nat. Mater. **12**, 605 (2013).

[55] W. Zhang, Z. Li, F. Li, H. Zhang, J. Peng, C. Tang, Q. Wang, K. He, X. Chen, L. Wang *et al.*, Phys. Rev. B **89**, 060506(R) (2014).

[56] J. He, X. Liu, W. Zhang, L. Zhao, D. Liu, S. He, D. Mou, F. Li, C. Tang, Z. Li *et al.*, Proc. Natl. Acad. Sci. U.S.A. **111**, 18501 (2014).

[57] S. Tan, Y. Zhang, M. Xia, Z. Ye, F. Chen, X. Xie, R. Peng, D. Xu, Q. Fan, H. Xu *et al.*, Nat. Mater. **12**, 634 (2013).

[58] J. Bang, Z. Li, Y. Y. Sun, A. Samanta, Y. Y. Zhang, W. Zhang, L. Wang, X. Chen, X. Ma, Q.-K. Xue *et al.*, Phys. Rev. B **87**, 220503(R) (2013).

[59] H.-Y. Cao, S. Tan, H. Xiang, D. L. Feng, and X.-G. Gong, Phys. Rev. B **89**, 014501 (2014).
[60] J. Shiogai, Y. Ito, T. Mitsuhashi, T. Nojima, and A. Tsukazaki, Nat. Phys. **12**, 42 (2016).
[61] B. Lei, J. H. Cui, Z. J. Xiang, C. Shang, N. Z. Wang, G. J. Ye, X. G. Luo, T. Wu, Z. Sun, and X. H. Chen, Phys. Rev. Lett. **116**, 077002 (2016).
[62] S. Zhang, J. Guan, X. Jia, B. Liu, W. Wang, F. Li, L. Wang, X. Ma, Q. Xue, J. Zhang *et al.*, Phys. Rev. B **94**, 081116(R) (2016).
[63] M. D. Watson, S. Backes, A. A. Haghighirad, M. Hoesch, T. K. Kim, A. I. Coldea, and R. Valenti, Phys. Rev. B **95**, 081106(R) (2017).
[64] H. Zhang, D. Zhang, X. Lu, C. Liu, G. Zhou, X. Ma, L. Wang, P. Jiang, Q.-X. Xue, and X. Bao, Nat. Commun. **8**, 214 (2017).
[65] M. Ashton, J. Paul, S. B. Sinnott, and R. G. Hennig, Phys. Rev. Lett. **118**, 106101 (2017).
[66] N. Mounet, M. Gibertini, P. Schwaller, D. Campi, A. Merkys, A. Marrazzo, T. Sohier, I. E. Castelli, A. Cepellotti, G. Pizzi *et al.*, Nat. Nanotechnol. **13**, 246 (2018).
[67] C. Ding, G. Gong, Y. Liu, F. Zheng, Z. Zhang, H. Yang, Z. Li, Y. Xing, J. Ge, K. He *et al.*, ACS Nano **13**, 10434 (2019).
[68] D. L. Feng and C. G. Zeng (private communications).